International Journal of Computer Assisted Radiology and Surgery (2020) 15:1225–1233
https://doi.org/10.1007/s11548-020-02181-4

ORIGINAL ARTICLE

Evaluation of a marker-less, intra-operative, augmented reality guidance system for robot-assisted laparoscopic radical prostatectomy

Megha Kalia[1,2] · Prateek Mathur[1] · Keith Tsang[1] · Peter Black[3] · Nassir Navab[2] · Septimiu Salcudean[1]

Received: 21 November 2019 / Accepted: 22 April 2020 / Published online: 5 June 2020

Abstract

Purpose Robot-assisted laparoscopic radical prostatectomy (RALRP) using the da Vinci surgical robot is a common treatment for organ-confined prostate cancer. Augmented reality (AR) can help during RALRP by showing the surgeon the location of anatomical structures and tumors from preoperative imaging. Previously, we proposed hand-eye and camera intrinsic matrix estimation procedures that can be carried out with conventional instruments within the patient during surgery, take < 3 min to perform, and fit seamlessly in the existing surgical workflow. In this paper, we describe and evaluate a complete AR guidance system for RALRP and quantify its accuracy.

Methods Our AR system requires three transformations: the transrectal ultrasound (TRUS) to da Vinci transformation, the camera intrinsic matrix, and the hand-eye transformation. For evaluation, a 3D-printed cross-wire was visualized in TRUS and stereo endoscope in a water bath. Manually triangulated cross-wire points from stereo images were used as ground truth to evaluate overall TRE between these points and points transformed from TRUS to camera.

Results After transforming the ground-truth points from the TRUS to the camera coordinate frame, the mean target registration error (TRE) (SD) was 4.56 ± 1.57 mm. The mean TREs (SD) in the x-, y-, and z-directions are 1.93 ± 1.26 mm, 2.04 ± 1.37 mm, and 2.94 ± 1.84 mm, respectively.

Conclusions We describe and evaluate a complete AR guidance system for RALRP which can augment preoperative data to endoscope camera image, after a deformable magnetic resonance image to TRUS registration step. The streamlined procedures with current surgical workflow and low TRE demonstrate the compatibility and readiness of the system for clinical translation. A detailed sensitivity study remains part of future work.

Keywords Augmented reality · Image guided surgery · Prostate surgery · Robotic surgery · Medical imaging

Introduction

Robot-assisted laparoscopic radical prostatectomy (RALRP) has become a standard treatment for organ-confined prostate cancer [3,12]. To avoid cancer recurrence, the primary goal of RALRP is to surgically remove all cancer. Yet, the reported rate of positive surgical margins, i.e., of incomplete removal of cancer, is high at 11–40% [17]. This is because surgeons face a delicate trade-off between removing all cancer and preserving critical anatomical structures, like neurovascular bundle (NVB), responsible for sexual function, and urinary sphincters, responsible for continence, surrounding the prostate.

The visualization of critical periprostatic structures, prostate boundary, and tumors during surgery by augmented reality (AR) systems can help optimize this trade-off by helping the surgeon make more informed decisions during the surgery.

Megha Kalia and Prateek Mathur are co-first authors and contributed equally to the manuscript.

✉ Megha Kalia
mkalia@ece.ubc.ca

✉ Prateek Mathur
pmathur@ece.ubc.ca

[1] Electrical and Computer Engineering, University of British Columbia, 2329 West Mall, Vancouver, BC V6T 1Z4, Canada

[2] Computer Aided Medical Procedures, Technical University of Munich, Boltzmannstraße 15, 85748 Garching bei München, Germany

[3] Vancouver Prostate Centre, Department of Urologic Sciences, University of British Columbia, Vancouver, BC V5Z 1M9, Canada

For example, a surgeon will not attempt to spare the nerves on the right lateral aspect of the prostate if the preoperative magnetic resonance imaging (MRI) volume, fused with the endoscope view, shows them a right anterior tumor adjacent to the nerve. At the same time, if the preoperative MRI, fused with the endoscope view, shows that there are no tumors on the left side of the prostate, the surgeon will attempt to spare the nerves on the left side. Therefore, several AR systems that overlay endoscope camera video with medical imaging have been proposed for RALRP.

In one proposed system, AR for robotic laparoscopic partial nephrectomy is performed by tracking an implanted object along with using ultrasound [5]. First, a calibration template (checkerboard pattern) is inserted into the surgical field view. Using laparoscopic ultrasound with another checkerboard pattern visible to the camera, the tumor is segmented. Another AR system for RALRP uses transurethral ultrasound and passive landmarks to display ultrasound images in the camera view [9]. Surgical needles with known geometries are implanted in the prostate and segmented in the ultrasound volume. Then, by visualizing at least four needles that are not coplanar in the camera image, a registration between transurethral ultrasound and laparoscopic camera is determined. A median root mean square error of 1.1 mm was reported on phantoms. Although promising, the major drawback of these systems is that they require an external registration object to align medical images to the camera frame. Using external calibration objects and tracking systems is not practical during most surgeries due to sterilization and biocompatibility issues and limited intracorporeal space at the surgical site, in which several instruments and the endoscope must fit. Moreover, additional steps are required as inserting a template or a marker into the body takes time and does not fit into the normal surgical workflow creating significant translational challenges for AR [10].

In [15], a RALRP guidance system was presented where the authors registered preoperative MRI with the patient by using transrectal ultrasound (TRUS). Several weeks before surgery, the patient undergoes a multi-parametric MRI examination. The prostate and tumors are delineated on the T2-weighted MRI volume by a radiologist. During surgery, a transrectal ultrasound (TRUS) is positioned into the patient using a specialized brachytherapy stepper that allows computer control of the TRUS rotation angle. The TRUS and da Vinci robot are registered using the procedure outlined in [1,11]. A TRUS volume is acquired by programming the TRUS to rotate for an intra-operative volume acquisition. The two volumes are deformably registered. The surgeon can control the TRUS angle using one of the da Vinci instruments. The same instrument is used to navigate the transverse/axial MRI images, shown along with a rendered prostate in a virtual scene alongside the endoscope view, in the da Vinci surgeon's console. Moreover, since the surgical tool was visible in both the virtual scene and the endoscope's camera image, it acts as a cue to draw similarities in both the views. The above system leverages the real-time imaging capability of TRUS, combined with the better resolution and soft-tissue contrast of MRI, to be able to image prostate cancer, along with important anatomy (bladder neck, prostate, urethra, rectum). While the system was evaluated in patients, it does not present an AR solution since neither the MRI nor the TRUS is presented as an overlay onto the endoscopic camera view.

Usually two additional calibrations are required to correctly overlay medical information on top of endoscope images. These two calibrations are: camera intrinsic transformation and the hand-eye transformation. Kalia et al. [8] presents a marker-less, real-time hand-eye transformation and the camera intrinsic estimation technique. The technique, unlike previous ones, does not require external calibration markers and does not require to taking the endoscope out of the patient's body [13,14]. Thus, it is attractive for intra-operative surgical augmented reality applications.

In this paper, we describe and evaluate a complete AR RALRP system that allows the overlay of the annotated MRI on top of the endoscope view. Our system, built upon the system described in [15], additionally contains camera intrinsic and the hand-eye estimation procedures described in [8]. Overall, after a preoperative MRI to intra-operative TRUS deformable registration step described in [15], our workflow solely uses the da Vinci surgical instrument to bring the intra-operative ultrasound imaging into the camera view, through a series of calibrations. In total, three transformations are determined by collecting a few data points in the surgical field of view. Therefore, all the calibration steps can be performed inside the patient without taking the endoscope out of the patient. Thus, the calibrations fit seamlessly in the existing RALRP workflow and overall take less than 2.5 min to perform. Moreover, for each calibration step, we provide the surgeon real-time visual feedback for visual assessment of accuracy of the calibrations. Thus, if the visual accuracy is not satisfactory, the surgeon could collect a few extra points within seconds. Providing the surgeon the autonomy and freedom to perform without having to interact with other personnel in the operating room further decreases the potential time lost due to miscommunication. Furthermore, in this paper we used a water bath, for evaluation of our proposed RALRP AR guidance system and quantifying overall target registration error (TRE) to bring the data points from the TRUS to the camera coordinate system.

This manuscript is arranged as follows. "Augmented reality guidance system overview" section provides an overview of the AR guidance system and explains the various phases of our pipeline and the details about the three transformation estimation steps, i.e., transformation to bring the data points from TRUS to da Vinci coordinate system, camera intrinsic matrix estimation, and hand-eye transformation to bring the

points from da Vinci endoscope end-effector to the camera coordinate system. Then, "Materials and methods" section provides a detailed explanation of the setup and the methods used for the evaluation, using a water bath. "Results" section provides the results of the evaluation and reports overall system error. "Discussion" and "Conclusion" sections provide discussion, conclusion, and future work.

Augmented reality guidance system overview

To streamline our proposed methods in the existing workflow and to minimize the time required to perform intra-operative calibrations, we divide our surgical guidance pipeline into three phases: "before surgery," i.e., before the day of the surgery, "beginning of surgery," and "during surgery." Other than camera intrinsic parameter estimation, all calibrations were carried out at the "beginning-of-surgery" phase. However, camera intrinsic parameter estimation procedure was divided among "before-surgery" and "beginning-of-surgery" phases. Before surgery, we prepared multiple-depth camera intrinsic matrix, where we performed multiple camera calibrations using checkerboards at fixed distances from the endoscope. To these data, we fit a degree-four polynomial. Then, during the "beginning-of-surgery" phase, the camera parameters were retrieved from this multiple-depth camera intrinsic matrix. The details are given in the following sections.

Before-surgery phase

In this phase, before surgery, the preoperative MRI of the patient is segmented to outline the prostate boundary and cancerous lesions. Also, to retrieve camera intrinsics during surgery, a multiple-depth camera intrinsic matrix was prepared before surgery, as described below.

Preoperative multiple-depth camera intrinsic matrix preparation

To perform multiple camera calibrations at various depths from the endoscope, we used a custom 3D-printed apparatus that can be mounted at the tip of the endoscope (Fig. 1b). The apparatus has a platform that can be accurately moved to fixed depths. For each level of depth, a checkerboard pattern was placed on the platform and camera calibration was performed after focusing the da Vinci endoscope. Thus, by using the apparatus, multiple repetitions of camera calibration can be done reliably, at a single distance from the endoscope. Checkerboards with different square sizes were used to perform the calibrations at different distances from the endoscope. The size of the square of the checkerboard was increased by 1 mm with each focal plane distance from the endoscope. To perform calibration at a particular distance, we placed the checkerboard pattern on the platform of the apparatus. Then, 25–30 different images of the checkerboard in different orientations were captured. These images were used to perform camera calibration at each level using the method described in [19]. These steps were repeated for all fixed depths from the endoscope. This entire procedure of performing camera calibration at each depth level was repeated five times. Therefore, we obtained the camera intrinsic parameters as a function of distance from the endoscope, to which a fourth-degree polynomial was fit. As opposed to the method proposed in [14], which requires a checkerboard image during surgery to estimate the camera intrinsic parameters, our method relies upon the distance from the endoscope to the instrument to retrieve the appropriate calibration parameters and can be carried out without disrupting surgical flow.

Beginning-of-surgery phase

In the second phase, at the beginning of surgery, the preoperative MRI is deformably registered to the volume obtained from an initial TRUS sweep [15]. Then, the TRUS is calibrated to the da Vinci robot to bring the TRUS volume into the kinematic frame of the robot. This step is followed by an intra-operative camera intrinsic retrieval and a hand-eye calibration step.

TRUS to da Vinci calibration

This is the first step of the AR pipeline for RALRP that brings TRUS into the kinematic frame of the da Vinci surgical robot. This allows control over the TRUS sweep angle using the da Vinci surgical tool. To calibrate, we used a procedure outlined in [1]. In this procedure, the surgeon palpates the surface of the prostate using the da Vinci surgical instrument. The corresponding point is located in the TRUS coordinate frame by rotating the transducer using the TRUS motor, until the surgical tool tip in the TRUS image is seen as a bright artifact at the air–tissue boundary. The tool tip is segmented manually in the TRUS coordinate frame. The corresponding tool tip location in the da Vinci kinematic frame is obtained via the da Vinci Research API [4]. This is repeated at least four times to obtain corresponding points at different locations on the prostate surface, typically at the prostate apex and base and three points along the midgland. Using an exhaustive search to remove outliers, the remaining points are used to calculate the homogeneous transformation ${}^{\mathrm{DV}}T_{\mathrm{TRUS}}$ between the two coordinate systems. This calibration typically takes less than 2 minutes.

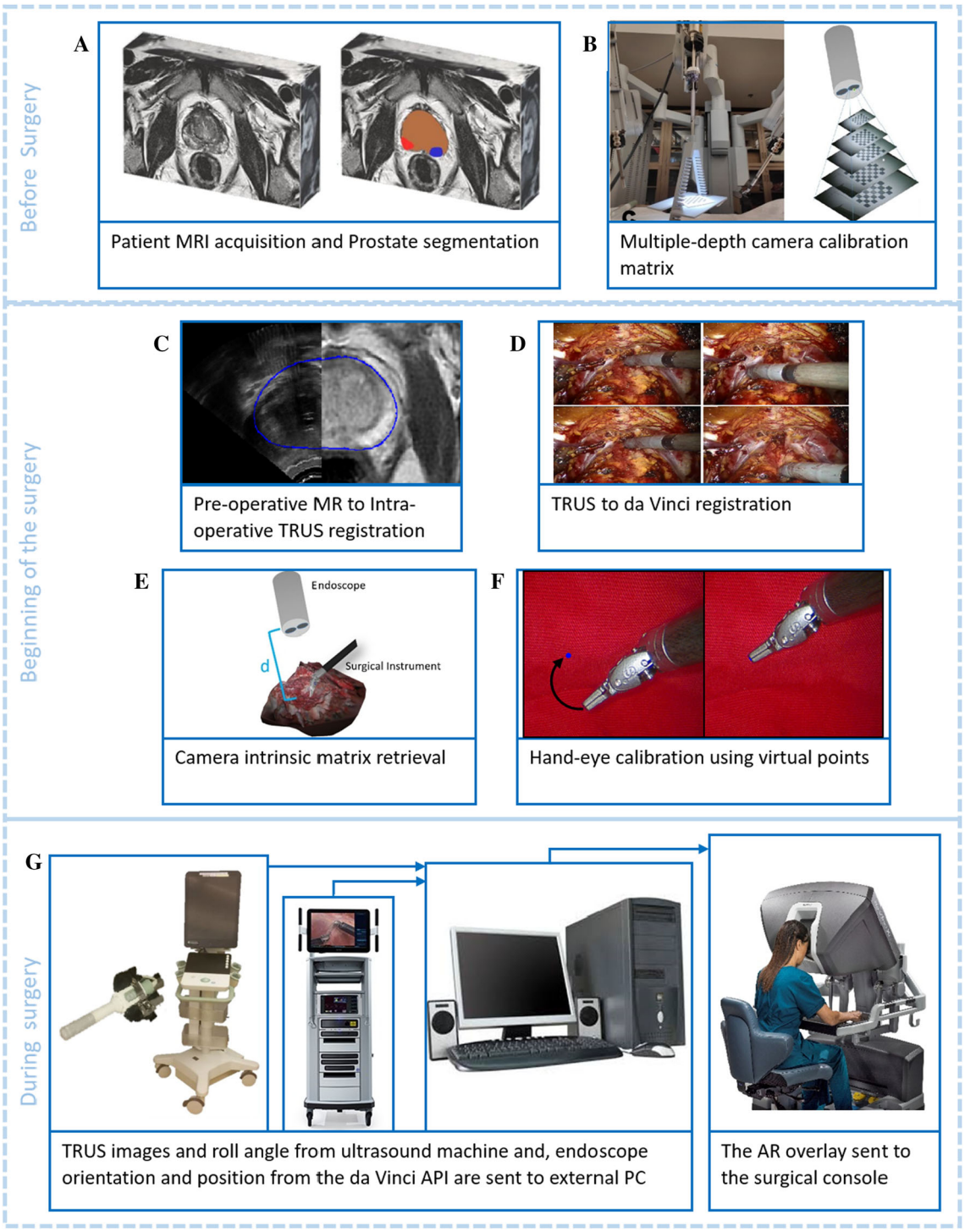

Fig. 1 Augmented reality system pipeline. **a** Preoperative MRI segmentation. **b** Camera calibration and multiple depths. **c** MRI–TRUS registration. **d** TRUS–da Vinci registration. **e** Camera intrinsic matrix retrieval from surgical depth estimation. **f** Hand-eye calibration. **g** Real-time AR updating

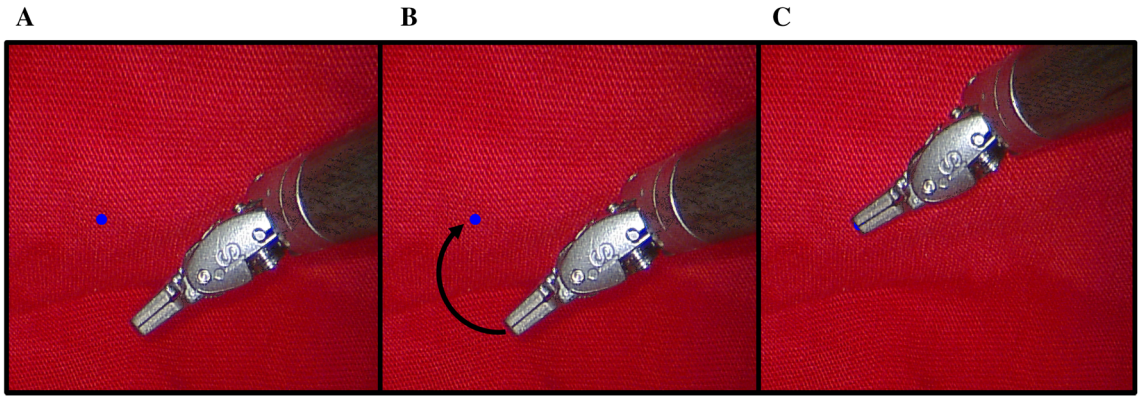

Fig. 2 **a** Difference between the rendered surgical instrument tip in blue and the actual surgical instrument tip without the hand-eye calibration. **b** Moving the surgical instrument tip to the incorrectly rendered tool tip, adding a data point to the hand-eye calibration. **c** Visual feedback of the calibrated tool tip

Intra-operative camera intrinsic matrix retrieval

During surgery, if the distance of the focal plane from the endoscope is known, the camera intrinsic parameters can be determined. To estimate the distance of the focal plane from the endoscope during surgery, we make a reasonable assumption that the location of the focal plane is where the surgeon is performing surgery and the surgical tools are located at that focal plane. To determine depth of the focal plane, the Euclidean distance between the endoscope end-effector and da Vinci tool tip is calculated using positions reported by the da Vinci Research API. We then retrieve the camera intrinsic parameters corresponding to that distance from our multiple-depth camera calibration matrix from the "before-surgery phase." This step takes less than 1s to perform.

Hand-eye: endoscope end-effector to camera calibration

Using endoscope end-effector position and orientation data from the da Vinci Research API, 3D points can be transformed from the robot base to the endoscope end-effector location with the transform ${}^{E}T_{\mathrm{DV}}$. It is important to note here that this is not the true camera location. To see the points in camera image and to facilitate AR, it is essential to bring the points in the camera coordinate frame from endoscope end-effector. Without this step, the rendered 3D points are seen at a different location in the image than the actual target, as shown in Fig. 2a. Thus, generally an additional transformation, known as the hand-eye transformation (${}^{C_L}T_E$), is required for accurate overlay of the medical data.

To estimate the hand-eye transformation, 3D points should be determined simultaneously, in both the endoscope end-effector and the camera coordinate frame. This is a challenging task during surgery and thus has remained an active area of research [2,13,16,18]. In [8], we proposed a hand-eye calibration step compatible with the existing intra-operative surgical workflow. In our approach, the surgical instrument tip position, obtained from the robot's forward kinematics via the da Vinci API, is rendered on screen without the hand-eye transformation. As shown in Fig. 2a, the erroneous rendered tool tip position is seen with an offset, along with the image of the actual surgical tool. Thus, as the surgeon moves the tool in the surgical field of view, the accuracy could be assessed visually. Wherever the visual error is large, the rendered surgical tip can be frozen by pressing a button and the surgeon is asked to move the surgical instrument tip to the rendered frozen dot. The surgeon carries out this step by bringing the tool tip to the location of the rendered dot in 3D. As soon as the surgeon meets the rendered 3D tool tip, the position of the surgical instrument tip is recorded in the endoscope end-effector frame from forward kinematics data, along with the image space coordinates of the rendered tool tip in left and the right endoscope camera images. We estimate the position of the surgical tool in the left camera coordinate frame using stereo triangulation. Then, the transformation between the camera and the endoscope end-effector coordinate frames is estimated by using an iterative gradient descent approach by minimizing the sum of squared residual (SSR). To estimate the transformation, we consider only those points where the visual offset between the true surgical tool tip and the rendered virtual surgical tool tip is high. The data points are added iteratively in the dataset. Since the transformation is estimated after the addition of every new point, the visual assessment for accuracy can be done after each point. To estimate the transformation, at least three corresponding point sets are required. However, if not satisfied with current visual accuracy, new points can be selected within seconds. This method does not require any external calibration markers, does not need an additional bed-side assistant, and can be performed in less than 30 seconds during surgery.

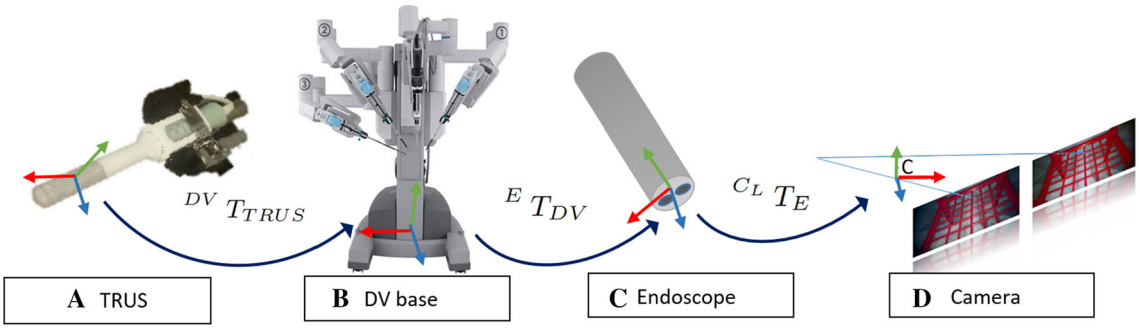

Fig. 3 The sequence of calibrations (**a**–**d**) involved in our AR guidance system, to bring the TRUS imaging to the endoscope camera frame. ${}^{\mathrm{DV}}T_{\mathrm{TRUS}}$ transforms points from TRUS to da Vinci, ${}^{E}T_{\mathrm{DV}}$ from da Vinci to endoscope, ${}^{C_L}T_E$ from endoscope to camera, and finally, K, camera intrinsic matrix (not shown) brings data points from the camera world to image space coordinates

Thus, the calibrations performed to bring the TRUS imaging data to the camera coordinate frame ${}^{i}T_{\mathrm{TRUS}}$ are as follows:

$$ {}^{i}T_{\mathrm{TRUS}} = K \times {}^{C_L}T_E \times {}^{E}T_{\mathrm{DV}} \times {}^{\mathrm{DV}}T_{\mathrm{TRUS}} \quad (1) $$

where ${}^{\mathrm{DV}}T_{\mathrm{TRUS}}$ is the TRUS to da Vinci transformation, ${}^{E}T_{\mathrm{DV}}$ is the da Vinci to endoscope end-effector transformation, ${}^{C_L}T_E$ is the endoscope to camera transformation, and K is the camera intrinsic matrix. The sequence of calibrations is also shown in Fig. 3.

During-surgery phase

During surgery, the AR visualization is updated by updating the endoscope and the surgical tool tip positions using data from the da Vinci Research API.

Materials and methods

The evaluation of our AR guidance system is not straightforward as a gold-standard method does not exist. Therefore, we designed an evaluation procedure to validate our proposed AR guidance pipeline. The following sections describe in detail our evaluation setup.

Hardware and software

We used the da Vinci Si system to perform and evaluate all the calibration steps. For TRUS imaging, we used a BK3500 ultrasound machine with the E14CL4b 14-4 MHz biplane transducer (BK Medical, Herlev, Denmark). The transducer was mounted to a robot controller motor also used in [11]. The motor allows for axial rotation of the ultrasound probe, controlling the sagittal ultrasound plane. To find the 3D points in the TRUS coordinate frame, we used custom-built software developed by the authors in [15]. The da Vinci Research API [4] was used to find the corresponding points in the da Vinci base coordinate system.

For the preparation of multiple-depth camera intrinsic matrix, various camera calibrations were performed using the MATLAB 2019a stereo camera calibration application. OpenGL version 4.5 was used to render the virtual scene. After processing, the right and left stereo video streams were sent back to the da Vinci console through SDI connections. To evaluate the overall registration error, a rigid cross-wire grid was designed in SolidWorks 2017 to provide targets visible in both camera and ultrasound.

Evaluation setup

To evaluate the overall registration error, i.e., the transformations from the TRUS to the camera coordinate frame, it is important to locate the corresponding points in both the camera and the TRUS coordinate frame. For this purpose, we used a water bath with cold water to avoid distortions in the image. We chose a water bath over a phantom (e.g., gelatin phantom) as the points inside the phantom, which are visible in TRUS, will be occluded by the phantom's surface in the camera image, preventing points from being chosen in both the coordinate systems simultaneously.

In order to do accurate point selection in both the coordinate systems, a rigid object is required with easily detectable features. A 3D-printed grid of 5 × 5 cross-wires with 1cm spacing was created. The cross-wires served as the reference points in both the camera and the TRUS coordinate systems.

We then submerged the grid in the water bath. The cross-wire points could easily be seen in the water bath as shown in Fig. 4. We selected each cross-wire in the ultrasound volume using our custom-made software mentioned before. Each trial, i.e., each grid position, resulted in 25 points. In order to collect points in the entire TRUS vol-

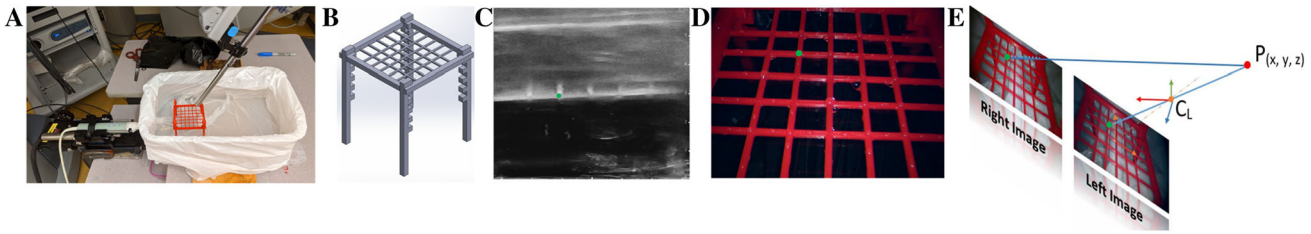

Fig. 4 **a** Evaluation setup with robotic ultrasound controller, water bath, da Vinci endoscope, and evaluation object. **b** CAD model of evaluation object. **c** Evaluation object with cross-wires visible in ultrasound. **d** Evaluation object with cross-wires visible in the camera view. **e** Stereoscopic triangulation of cross-wire points to establish ground truth. Green dot in subfigures **c**–**e** corresponds to same cross-wire point on the evaluation object

Table 1 Mean TRE error of TRUS data points

n	error_x	error_y	error_z	$\text{error}_{\text{total}}$
Top (35)	2.50 ± 1.42 mm	1.30 ± 1.09 mm	2.12 ± 1.46 mm	3.97 ± 1.39 mm
Middle (105)	1.87 ± 1.20 mm	1.74 ± 1.11 mm	3.16 ± 1.93 mm	4.51 ± 1.61 mm
Bottom (35)	1.58 ± 1.10 mm	3.53 ± 1.16 mm	3.02 ± 1.70 mm	5.25 ± 1.39 mm

ume and the surgical field of view, the grid was placed in different orientations and at different depths between trials. We covered the entire volume in seven trials. To estimate the corresponding points in the camera coordinate system, after each trial the water was drained out to remove the effect of refraction from the water on the camera image. While doing so, the grid object was kept stationary. Then, the right and left endoscope camera images were captured.

To generate a validation dataset, we used stereo triangulation on left and right camera images to determine the world positions of grid points in the left camera coordinate frame. This step was preceded by a camera calibration step using a checkerboard. We used these points as ground truth and calculated the overall error using these points. All the calibrations were performed in the sequence described in equation 1 and by the procedures described in "Augmented reality guidance system overview" section, except for the ${}^{\text{DV}}T_{\text{TRUS}}$ estimation procedure where we used a surgical glove filled with water to mimic the air–tissue boundary. After the calibration steps, the TRUS points were brought to the camera coordinate frame. Then, we calculated TRE as the Euclidean distance between these transformed TRUS points and the ground-truth points in the camera coordinate system.

Results

The re-projection error of the camera calibration, in a 1920×1080 pixel image, was 1.2 pixels. The re-projection error of stereo triangulated ground-truth points in the camera coordinate space came out to be 5.99 pixels. We collected 175 points by placing the grid at multiple locations in the field of view. After removing the outliers, we had 166 data points. The mean overall TRE (SD) was 4.56 ± 1.57 mm, with maximum and minimum TRE of 7.92 mm and 2.45 mm, respectively. The individual mean (SD) TRE in x-, y-, and z-directions was 1.93 ± 1.26 mm, 2.04 ± 1.37 mm, and 2.94 ± 1.84 mm, respectively. With the intention to identify any region-based variability, we also analyzed the data points based on their locations in the image. Here, different locations of the points in the image correspond to the different locations of these points in the TRUS volume and the camera viewing volume. We divided the cross-wire points in the top, middle, and bottom regions with the total number of points as 35, 105, and 35, respectively, in each region. The mean TRE for different regions is summarized in Table 1.

Discussion

We obtained an overall mean TRE of 4.56 mm. In clinical terms, this error should be small enough to accurately delineate important periprostatic structures. For example, the NVB lies roughly 3 mm from the posterolateral aspect of the prostate [7]. If the tumor is located in the posterolateral region of the prostate, the required accuracy of the AR system must be around 3 mm. In cases where the cancer is located more medially, however, our system can help the surgeon make decisions on whether to perform nerve-sparing techniques or to be more aggressive in their dissection.

Furthermore, although it is not easy to draw direct comparisons, a method was proposed in [5], where using

checkerboard patterns on the ultrasound and an implanted object, the authors transformed the segmented tumor from ultrasound to the implanted object's kinematic frame and then to the camera. They reported an overall system error of 5.1 mm. This is comparable to our system, even though we do not require an intra-operative calibration template. Furthermore, the authors of [9] report an error of 1.1 mm. Their system consisted of transurethral ultrasound and surgical needles to act as fiducials for registration of ultrasound to the endoscope. While the reported error is impressive, they do not report their endoscope calibration error, which is an important step in enabling AR. Overall system error may actually be comparable to our system. The main advantage to our proposed system compared to these methods is that it does not require an external calibration object, streamlining the intra-operative workflow.

The mean TRE in z-direction, i.e., the viewing direction in the endoscope, is greater than mean TRE in x- and y-directions. This finding is similar to the results of our previous study [8], evaluating the accuracy of our hand-eye calibration method. Since the hand-eye calibration is a part of our overall calibration pipeline, this error might be introduced by the hand-eye calibration procedure. For the hand-eye calibration, one source of high error in z-direction could be the smaller baseline of the stereo endoscope ($\approx$ 5 mm). It is well known that the depth perception resolution is inversely proportional to the baseline distance. In future, it will be interesting to look into the possible intra-operative approaches to minimize the TRE in the z-direction.

Furthermore, the TRUS to da Vinci calibration, intra-operative camera intrinsic retrieval, and the hand-eye calibration steps took ≈ 30 s, < 1 s, and ≈ 30 s, respectively, to perform. Thus, our methods are highly suitable for any real-time intra-operative application.

For the TRUS to da Vinci calibration step, we select at an average four points, and for the hand-eye calibration, the average of three points give satisfactory visual accuracy. However, at any point if the user is not satisfied with the visual accuracy, more points can be added to estimate each of the calibrations.

Additionally, as part of the evaluation procedure, to estimate the positions of the cross-wire points in the TRUS coordinate system, we manually selected the points in the TRUS image. Although care was taken to select the center most point of the cross-wire, errors might have introduced inadvertently during this step. In the future, to make this step user independent, we plan to implement an approach similar to [6] to automate the localization of the surgical tool in the US image. Furthermore, in its current form, both our calibration procedures, i.e., TRUS to da Vinci robot and the hand-eye calibration, require a user to manually select data points. Thus, the steps are user dependent. Therefore, in the future, we plan to do a more extensive evaluation with more users. Furthermore, when analyzing results based on the points' location in the camera, errors closer to the camera were larger than those at a greater distance. This may arise from inaccurate point segmentation in ultrasound, as we did a manual segmentation. The way the setup was oriented, in some trials, the cross-wires were at the distal end of the ultrasound imaging plane. There may be inaccuracies in ultrasound reconstruction at the edges of the image, causing inaccuracies in segmentation.

Conclusion

In this paper, we present the evaluation of an intra-operative, marker-less, real-time AR guidance system for RALRP. We also reported overall TRE to bring the data points from intra-operative TRUS to the camera coordinate system. The system is built upon the one proposed in [15] and includes two additional transformations, i.e., camera intrinsic matrix and the hand-eye transformation. The transformations can be estimated by collecting a few data points using the surgical instrument already visible in the endoscope and thus fit effortlessly with the previously proposed methods. Overall, our AR system involves estimating three transformations: from TRUS to the da Vinci base coordinate system, the camera intrinsic matrix, and the hand-eye transformation. For evaluating the entire chain of calibrations, a 3D-printed cross-wire was made visible in TRUS and stereo endoscope by placing in a water bath. Then, cross-wire points were manually selected in the endoscope right and left images for triangulation, to bring in the points in left camera coordinate frame. This was used as ground-truth dataset. Then, corresponding points in TRUS coordinate were transformed to the camera coordinate frame after applying all the sequence of transformations. Overall TRE was calculated between transformed points and the ground-truth points, in the camera coordinate frame, by calculating the Euclidean distance between the two.

The overall reported error can be reduced further at any point of the procedure by selection of new US and camera points. As the tool tip is always visible, our technique provides a safe, quick, and verifiable method for ultrasound to camera registration. Thus, our proposed method is aligned with the current RALRP procedure with minimal changes to the existing workflow. Moreover, although we have proposed our methods for prostate surgery, any surgery that utilizes US guidance (e.g., kidney, liver, neck, etc.) can benefit from our proposed calibration methods.

Acknowledgements The authors are thankful for financial support provided by the Canadian Institutes of Health Research (CIHR), the Natural Sciences and Engineering Research Council (NSERC), and the Charles Laszlo Chair in Biomedical Engineering held by Professor Salcudean. The authors thank the Canadian Research Chairs (CRC) and Canada Foundation of Innovation (CFI) for their support. The authors would also like to thank Intuitive Surgical for providing the research API and support.

Compliance with ethical standards

Conflict of interest The authors declare that they have no conflict of interest.

Ethical standard This article does not contain any studies with human participants or animals performed by any of the authors.

Informed consent This article does not contain patient data.

References

1. Adebar T, Salcudean S, Mahdavi S, Moradi M, Nguan C, Goldenberg L (2011) A robotic system for intra-operative trans-rectal ultrasound and ultrasound elastography in radical prostatectomy. In: Taylor RH, Yang GZ (eds) Information processing in computer-assisted interventions. Springer, Berlin, pp 79–89
2. Chen EC, Morgan I, Jayarathne U, Ma B, Peters TM (2017) Hand-eye calibration using a target registration error model. Healthc Technol Lett 4(5):157–162
3. Cooperberg MR, Lubeck DP, Meng MV, Mehta SS, Carroll PR (2004) The changing face of low-risk prostate cancer: trends in clinical presentation and primary management. J Clin Oncol 22(11):2141
4. DiMaio S, Hasser C (2008) The da Vinci research interface. MIDAS J. http://hdl.handle.net/10380/1464
5. Edgcumbe P, Singla R, Pratt P, Schneider C, Nguan C, Rohling R (2016) Augmented reality imaging for robot-assisted partial nephrectomy surgery. In: International conference on medical imaging and augmented reality. Springer, pp 139–150
6. Groves L, Vanberlo B, Peters T, Chen E (2019) A deep learning approach for automatic out-of-plane needle localization for semi-automatic ultrasound probe calibration. Healthc Technol Lett 6:204–209
7. Inoue S, Shiina H, Hiraoka T, Mitsui Y, Sumura M, Urakami S, Igawa M (2009) Retrospective analysis of the distance between the neurovascular bundle and prostate cancer foci in radical prostatectomy specimens: its clinical implication in nerve-sparing surgery. BJU Int 104(8):1085–1090
8. Kalia M, Mathur P, Navab N, Salcudean T (2019) A marker-less real time intra-operative camera and hand-eye calibration procedure for surgical augmented reality. Healthc Technol Lett 6:255–260
9. Lanchon C, Custillon G, Moreau-Gaudry A, Descotes JL, Long JA, Fiard G, Voros S (2016) Augmented reality using transurethral ultrasound for laparoscopic radical prostatectomy: preclinical evaluation. J Urol 196(1):244–250
10. Linte CA, Davenport KP, Cleary K, Peters C, Vosburgh KG, Navab N, Jannin P, Peters TM, Holmes DR III, Robb RA (2013) On mixed reality environments for minimally invasive therapy guidance: systems architecture, successes and challenges in their implementation from laboratory to clinic. Comput Med Imaging Graph 37(2):83–97
11. Mohareri O, Ischia J, Black PC, Schneider C, Lobo J, Goldenberg L, Salcudean SE (2015) Intraoperative registered transrectal ultrasound guidance for robot-assisted laparoscopic radical prostatectomy. J Urol 193(1):302–312
12. Novara G, Ficarra V, Rosen RC, Artibani W, Costello A, Eastham JA, Graefen M, Guazzoni G, Shariat SF, Stolzenburg JU, Van Poppelk H, Zattonia F, Montorsil F, Mottrieb A, G. Wilson T (2012) Systematic review and meta-analysis of perioperative outcomes and complications after robot-assisted radical prostatectomy. Eur Urol 62(3):431–452
13. Pachtrachai K, Allan M, Pawar V, Hailes S, Stoyanov D (2016) Hand-eye calibration for robotic assisted minimally invasive surgery without a calibration object. In: 2016 IEEE/RSJ international conference on intelligent robots and systems (IROS). IEEE, pp 2485–2491
14. Pratt P, Bergeles C, Darzi A, Yang GZ (2014) Practical intraoperative stereo camera calibration. In: International conference on medical image computing and computer-assisted intervention. Springer, pp 667–675
15. Samei G, Tsang K, Kesch C, Lobo J, Hor S, Mohareri O, Chang S, Goldenberg SL, Black PC, Salcudean S (2019) A partial augmented reality system with live ultrasound and registered preoperative MRI for guiding robot-assisted radical prostatectomy. Med Image Anal 60:101588
16. Shao J, Luo H, Xiao D, Hu Q, Jia F (2017) Progressive hand-eye calibration for laparoscopic surgery navigation. In: Cardoso J, Arbel T, Luo X, Wesarg S, Reichl T, González Ballester MÁ, McLeod J, Drechsler K, Peters TM, Erdt M, Mori K, Linguraru MG, Uhl A, Oyarzun Laura C, Shekhar R (eds) Computer assisted and robotic endoscopy and clinical image-based procedures. Springer, New York, pp 42–49
17. Silberstein JL, Eastham JA (2014) Significance and management of positive surgical margins at the time of radical prostatectomy. Indian J Urol IJU J Urol Soc India 30(4):423
18. Thompson S, Stoyanov D, Schneider C, Gurusamy K, Ourselin S, Davidson B, Hawkes D, Clarkson MJ (2016) Hand-eye calibration for rigid laparoscopes using an invariant point. Int J Comput Assist Radiol Surg 11(6):1071–1080
19. Zhang Z (2000) A flexible new technique for camera calibration. IEEE Trans Pattern Anal Mach Intell 22:1330–1334